Carlos Alberola, S.; Sanchez Saez, F.; Martorell Alsina, SS. (2014). Use of TRACE best estimate code to analyze spent fuel storage pools safety. Progress in Nuclear Energy. 77:224-238. doi:10.1016/j.pnucene.2014.07.008.

Use of TRACE best estimate code to analyze spent fuel storage pools safety

S. Carlos [a,*], F. Sanchez-Saez [a], S. Martorell [a]

[a] *Departament d'Enginyeria Química i Nuclear, Universitat Politècnica de València. Cami de Vera, 14. València. Spain.*

Abstract

Nuclear policies have experienced an important change since Fukushima Daiichi nuclear plant accident and the safety of spent fuels has been in the spot issue among all the safety concerns. At many countries, the spent fuel of nuclear power plants is not reprocessed so it has to be stored inside the facilities, normally in pools. As nuclear power plants use best estimate codes to perform safety analysis, it is interesting to assess the capacity of such codes to simulate spent fuel pools behavior. This paper uses TRACE thermal-hydraulic code to simulate steady state and transient conditions of spent fuel pools. The steady state results are compared with plant measurements of Maine Yankee with a good agreement between the calculations and the measurements. The transient simulated is a loss of cooling together with a loss of coolant through the transfer channel. TRACE heat transfer radiation model has been activated using the parameters obtained from COBRA thermal-hydraulic code.

Key words: spent fuel pool, TRACE, loss of cooling, loss of coolant, RADGEN, COBRA.

1 Introduction

Nuclear policies have experienced an important change since March 11 of 2011, when an earthquake and the following tsunami caused the loss of adequate cooling capability of the reactors and spent fuel pools of Fukushima Daiichi nuclear plant in Japan. Accordingly, the safety of spent fuels has been in the spot issue among all the safety concerns (Hung et al. , 2013).

* Corresponding author.
Email addresses: scarlos@iqn.upv.es (S. Carlos), frasansa@etsii.upv.es (F. Sanchez-Saez), smartore@iqn.upv.es (S. Martorell).

In Spain, nuclear energy is being used for commercial use since the 80's and until now most of the spent fuel assemblies are stored in the spent fuel pools inside the plant. As in other countries (Lee and Lee , 2007), spent fuels are not reprocessed and most of the spent fuel pools are near their maximum capacity. This is one of the reasons why the Spanish government approved the construction of a centralized installation to store the spent fuel assemblies of all the Spanish nuclear reactors (Rogers , 2009). However, the construction of such installation is now in the earliest phase and Spanish nuclear plants have to store their spent fuels in safe conditions until the project is completed. So the evaluation of spent fuels pools safety becomes of great importance in accessing the magnitude of effects following a nuclear accident.

Fukushima's accident evidenced the need of identifying and analyzing the possible accidental sequences in the spent fuel pools. In fact, such sequences are already identified, and in references (Throm , 1989) and (Ibarra et al. , 1997) a probabilistic risk assessment of each one of them is performed. In such references, the loss of cooling capacity and/or the loss of spent fuel coolant inventory are identified as possible accidental sequences that could take place in the spent fuel pool, and some examples of incidents occurred in commercial nuclear power plants related with the loss of cooling capacity and/or coolant are encountered in reference (Throm , 1989).

In order to improve the spent fuel pools safety analysis, it is of great interest to analyze the deterministic safety of the sequences considered as most important. Several thermal-hydraulic studies on spent fuel pools safety can be found in the literature. For example, a computational fluid dynamics (CFD) approach has been used in (Hung et al. , 2013) to evaluate spent fuel pool behavior after the loss of the cooling capability to remove the decay heat and after the complete loss of spent fuel pool coolant inventory. The capability of CFD to simulate three dimensional and two phase phenomena is an advantage to evaluate the evolution the transient inside the spent fuel pool, but it is very demanding from the computational point of view. In other studies as, for example, in references (Gay and Gloski , 1983) and (Gay , 1984) the authors develop GFLOW code to perform a thermal-hydraulic study of Maine Yankee spent fuel pool and the results obtained are compared with measured data and with the values predicted by the results provided by RELAP-4 best estimate code.

In fact, the use of best estimate codes can be interesting in spent fuel pool transient simulation because such codes have been used since the beginning of nuclear power plants operation to simulate accidental sequences, playing an important role to improve the knowledge about the physical phenomena that take place inside the reactor during a certain transient. Some of the codes used in such simulations are RELAP-5, TRAC, CATHARE, ATHLET or TRACE. At the beginning, these codes were developed and used to perform simulations

at full power conditions but, as some accidents have occurred at other modes of operation, they have also been used to simulate other kind of transients. For example, the loss of the RHR during shutdown in different plants, has been simulated using best-estimate codes such as RELAP-5 (Hassan and Raja , 1993), (Hassan and Banerjee , 1994), (Ferng and Ma , 1996), (Carlos et al. , 2008), (Villanueva et al. , 2008), CATHARE (Hassan and Troshko , 1997), TRAC-BF1 (Watanabe et al. , 2012).

In general, all of the transients simulated focus on the analysis of the reactor core behavior, but the experience gained in the best estimate code modeling and simulation can be useful to analyze the spent fuel pool thermal-hydraulic behavior.

Among these codes, RELAP-5 and TRAC have traditionally been used to reproduce transients of Pressurized Water Reactors (PWR) and Boiling Water Reactors, respectively. Nowadays, TRACE code (TRAC/RELAP Advanced Computational Engine) is being developed to make use of the most favorable characteristics of RELAP-5 and TRAC codes to simulate both, PWR and BWR, technologies. This code is nowadays being studied and it has been used in some interesting analyses as (Wang et al. , 2009) and (Vihavainen et al. , 2010).

Among the characteristics of TRACE code, the hydraulic component VESSEL can be useful to model spent fuel pools. Thus, as VESSEL is a three dimensional thermal-hydraulic component, it is interesting to take advantage of this feature to evaluate the physical phenomena present in the spent fuel storage pool, as in this case three-dimensional phenomena can be relevant for the results of the calculations (USNRC , 2010a) (USNRC , 2010b). Some works can be found in literature in which best estimate codes are used to analyze fuel storages. As it has been said before, in reference (Gay , 1984) RELAP-4 code is used to model Maine Yankee spent fuel storage pool. The results of the calculations performed were used by Yankee Atomic Electric Company to perform the spent fuel licensing thermal analysis. In (Gay , 1984), the model is constructed by dividing the spent fuel pool into different sections, each one of them is modeled using a PIPE component providing acceptable results. Nevertheless, PIPE component only simulates the fluid behavior in one dimension, so what happens in the other dimensions is missed. In reference (Kaliatka et al. , 2010), the results of the loss of heat removal accident for all the spent fuel pools at Ignalina nuclear power plant are presented. In this work a model for RELAP-5 to simulate the spent fuel pools is used to analyze the evolution of water evaporation and spent fuel uncovering. Finally, in (Wang et al. , 2012), the loss of cooling in Chinshan nuclear power plant is simulated using FLUENT and TRACE codes.

In this paper, a model of Maine Yankee nuclear power plant spent fuel pool

based on a VESSEL component is developed. This model is constructed to verify the capability of TRACE code to simulate the thermal hydraulic conditions which occur in an existing spent nuclear fuel storage pool, so the results provided are compared with experimental data. A calculation of the licensing case, where it is assumed that the pool is working under the worst possible operation conditions, was made and the results had been compared with GFLOW code results. And finally, assuming the heat load corresponding to the licensing case, a loss of cooling and loss of coolant transient is simulated considering the effect of thermal radiation.

The paper is organized as follows: In section 2, a description of Maine Yankee spent fuel pool is presented, the TRACE model developed for this spent fuel storage and the results obtained with this model are discussed. In section 3, a methodology to obtain thermal radiation model parameters based on the ones obtained using RADGEN code is explained. Section 4 presents the results obtained for a of loss of cooling and loss of coolant transient, and the differences of considering or not the thermal radiation. Finally, section 5 presents the main conclusions obtained.

2 Maine Yankee spent fuel pool

In order to verify the TRACE code capability to model a spent fuel pool the best option is to simulate an application and compare, the results calculated by the code with experimental data. References (Gay and Gloski , 1983) and (Gay , 1984) provide measured data of temperatures for Maine Yankee spent fuel pool, so in this work the results calculated by TRACE code using a model based on a VESSEL component are compared with the ones presented in these references.

Fig. 1 and Fig. 2 show the side and top views of Maine Yankee spent fuel pool, respectively. In Fig. 1 the position of the spent fuel at the bottom of the pool can be observed. The residual heat produced by the spent fuel is removed by injecting cold water at 3.96 m below the maximum pool water level, which is heated by the heat generated by the fuel assemblies and extracted at two different levels to be cooled and injected again. Fig. 2 shows the top view, (X-Y plane) of Main Yankee spent fuel pool. In this Figure, the position of all the racks in which the spent fuel can be placed is shown. It can be observed that the racks present different dimensions, what means that the number of fuel elements is not uniformly distributed inside the pool; therefore the residual heat generated is not equally distributed. Also in this Figure it is observed a zone between the fuel and the pool walls, which acts as a downcomer when natural circulation is established in the pool.

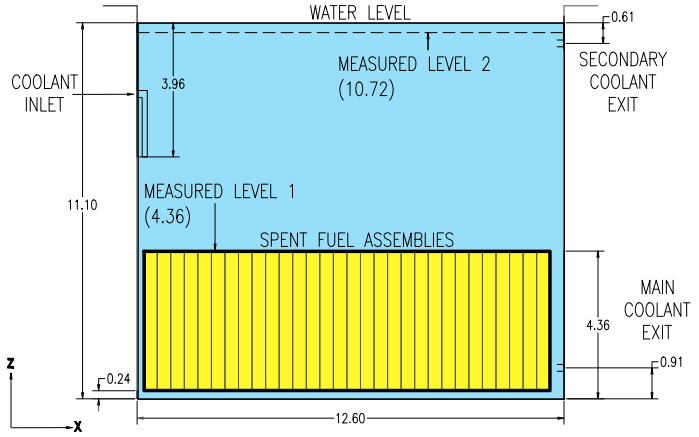

Fig. 1. Side View of Maine Yankee spent fuel storage pool.

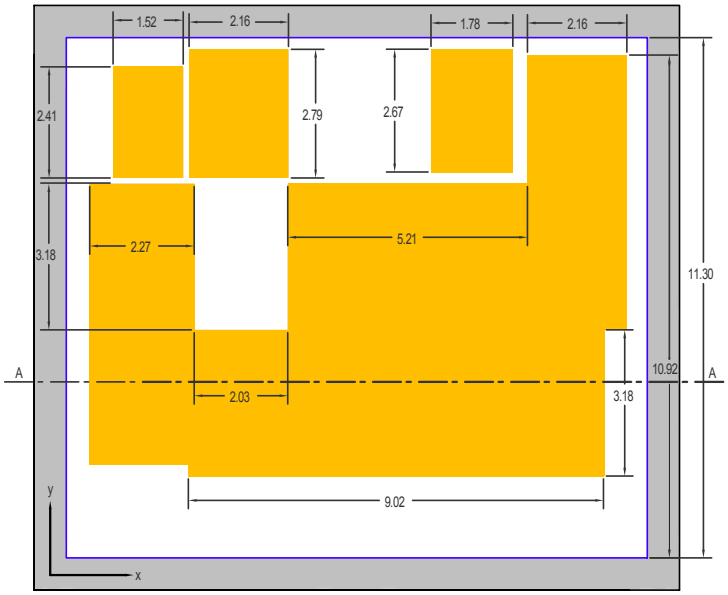

Fig. 2. Top View of Maine Yankee spent fuel storage pool.

The values of temperature have been measured at Maine Yankee spent fuel storage pool twenty-five days after reactor shutdown and with the full core offloaded into the pool (Gay and Gloski , 1983) and (Gay , 1984). The rest of the pool was filled with spent fuel assemblies that had been in storage between 1.5 and 9 years. A view of the location of the different kind of spent fuel elements in the pool is shown in Fig. 3. The amount of residual power generated by each cycle is presented in Table 1.

In this situation, the inlet mass flow was 98 kg/s at a temperature of 299.1 K. Coolant exited the pool through two separate locations (see Fig. 1), and it was not possible to determine the fraction of coolant passing through each one of the two possible exit locations. The top exit location was at a depth

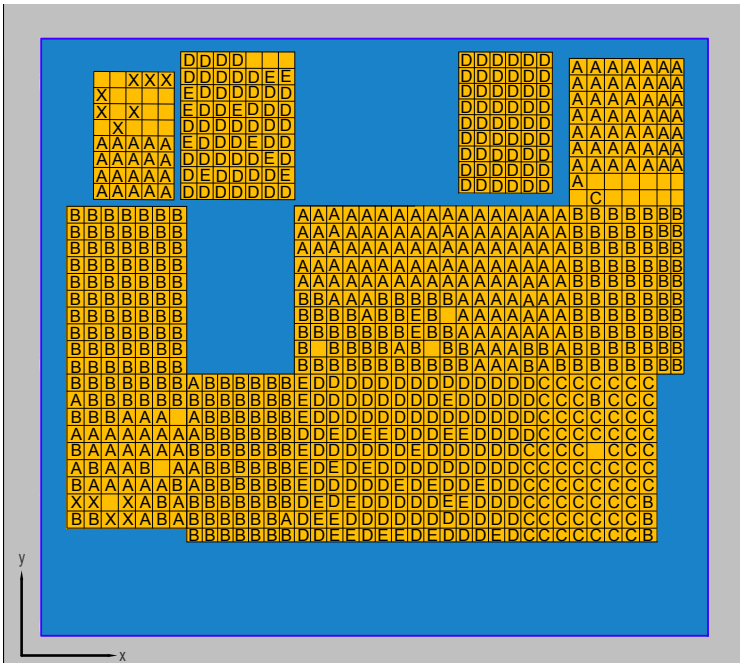

Fig. 3. Storage Rack Locations in Maine Yankee Spent Fuel Storage Pool.

Table 1
Power of the different fuel elements.

Symbol	Meaning	POWER (MW)
A	Cycle 1, 1a Fuel	0.025
B	Cycle 2, 3 or 4 Fuel	0.084
C	Cycle 5 Fuel	0.087
D	Cycle 6 Fuel	3.304
E	New Fuel	0.000
X	Core Internals	0.000

of approximately 0.76 m, and a temperature of 309.8 K was recorded at this location. The bottom suction was located at elevation of 0.91 m, where the measured temperature was 307.5 K.

2.1 Trace Model for Maine Yankee spent fuel storage pool

Maine Yankee spent fuel storage pool TRACE model is performed using a VESSEL hydraulic component (USNRC , 2010a) (USNRC , 2010b). This component allows to simulate a three dimensional flow calculation in (x, y, z) Cartesian and/or (r, θ, z) cylindrical geometry. For the nodalization of the spent fuel pool the Cartesian representation has been selected. The TRACE model developed has been constructed using Symbolic Nuclear Analysis Pack-

age (SNAP) (Applied Programming Technology, 2012), and is presented in Fig. 4. As boundary conditions, FILL 121 simulates the coolant injection into the spent fuel pool, BREAK 800 simulates the spent fuel pool building and BREAK 122 represents the main coolant outflow. The secondary coolant exit is not included in the model, because the measurement of the coolant temperature at the inlet of the heat exchanger and at the main coolant exit are the same, what means that the major part of the coolant is coming out the spent fuel pool by the main coolant exit (Gay and Gloski , 1983) (Gay , 1984).

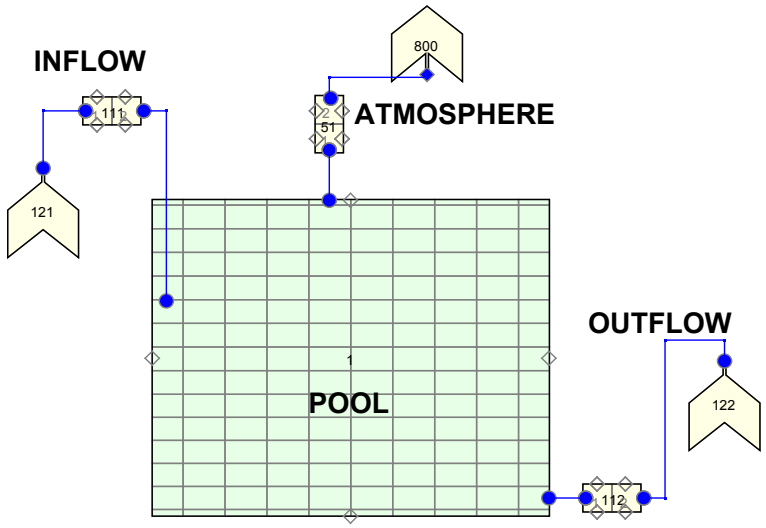

Fig. 4. TRACE model of the Maine Yankee Spent Fuel Pool.

The VESSEL component is of dimensions $(X, Y, Z) = (10, 10, 15)$ what results in 1500 cells. In axial direction, the first level, $Z = 1$, represents the pool lower plenum. The heated zone comprises from $Z = 2$ to $Z = 6$, above the fuel elements, from $Z = 7$ to $Z = 14$, the pool is full of water. Cells from $Z = 15$ and above are full of air, what simulates the spent fuel pool building.

The residual power generated by the fuel assemblies has been distributed inside the pool as detailed in references (Gay and Gloski , 1983) and (Gay , 1984), and following the power generation presented in Fig. 3 and Table 1. The latest discharged core generates 3.3 MW and the other assemblies generate 0.2 MW. All this power is distributed in different HEAT STRUCTURE components associated with the hydraulic cells of the VESSEL that represent the fuel assemblies. Thus, for each cell the number and cycle of the fuel assemblies are identified and the total residual power generated is computed and assigned to its associated HEAT STRUCTURE .

As part of the residual heat generated by the spent fuel assemblies is transferred to the spent fuel pool walls, this element was considered in the model as a HEAT STRUCTURE component, without power generation, using the ma-

terial data provided in reference (IAEA , 2007), considering the wall a width of 0.7 m of baritic concrete.

In normal operation, the spent fuel pool cooling circuit injects a coolant mass flow rate of 98 kg/s and with a temperature of 299.1 K to maintain a safe temperature value. Such injection is produced throughout PIPE 111 at axial level $Z = 10$ in the TRACE model to adjust the elevation to values exposed in Fig. 1. Finally, PIPE 112 and BREAK 122 represent the coolant exit.

2.2 Steady state calculation

Using the model presented in section 2.1, a TRACE calculation for the steady state has been performed and compared with the measured data from references (Gay and Gloski , 1983) and (Gay , 1984). Thus, Fig. 5 and Fig. 6 show the measured and TRACE prediction of coolant temperatures just above the fuel assemblies, respectively. Such temperatures were taken at 4.36 m of axial level, corresponding to the measure level 1 at Fig. 1.

TRACE calculates the temperature values in the center of the cell, so to better compare the calculations with the temperature measured by the thermocouples, an interpolation of TRACE temperatures has been performed to obtain the values in the same location as the measurements, which are presented in Fig. 5. The error between the measures and the calculations have been performed in each position and the largest deviation found is 0.76%, located near the inlet coolant (inside a circle in Fig. 5 and Fig. 6). At this location, the temperature measured is a mixture of the cold inlet mass flow and the hot temperature inside the spent fuel pool, while for TRACE it is closer to the cold water as the center of the cell is near to this location. The minimum error calculated is 0% (inside a square in Fig. 5 and Fig. 6), as the calculated temperature is exactly the same as the one provided by the measurement. Finally, the average error found is of 0.21%, what indicates good agreement between TRACE calculations and measured data is observed.

In Fig. 7 and Fig. 8, the measured and calculated temperatures are shown for a higher axial level, 10.72 m from the bottom of the spent fuel pool above the coolant injection (measured level 2 of the Fig. 1). At this level, the water temperature is more homogeneous and closer to the experimental value as no injection of cold water is produced. This is quantitatively observed with the average error calculation, which in this case is 0.075%, lower than the one obtained for locations near the spent fuel pool bottom. The maximun error found is 0.13% and the minimum error is 0.032%, marked inside a circle and a square in inside Fig. 7 and Fig. 8, respectively.

It is also interesting to study the temperatures in the X-Z plane at $Y = 4$, what

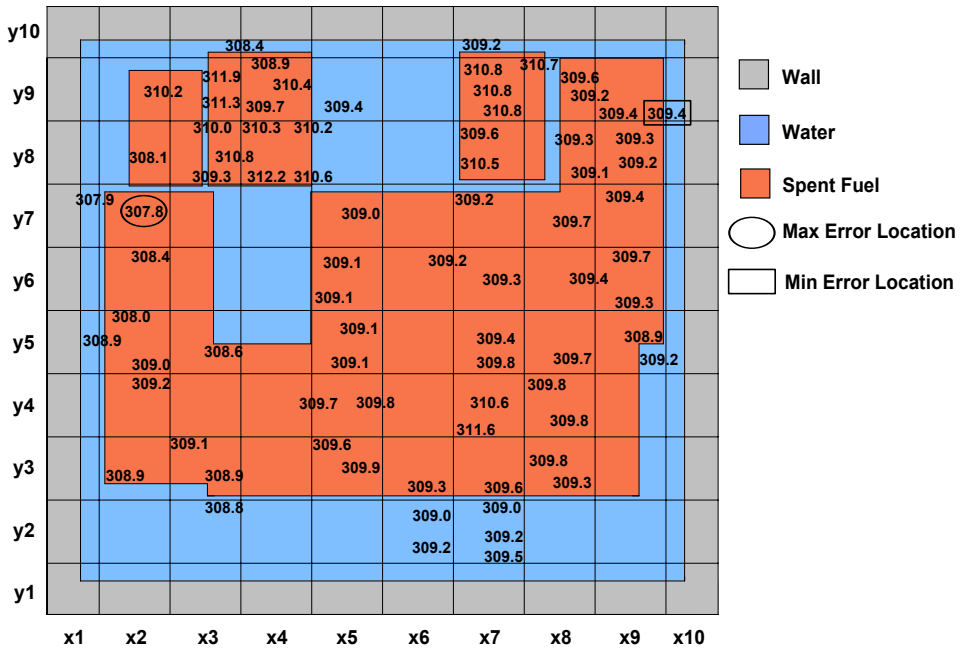

Fig. 5. Measured temperatures (K) at 4.36 meters from the bottom.

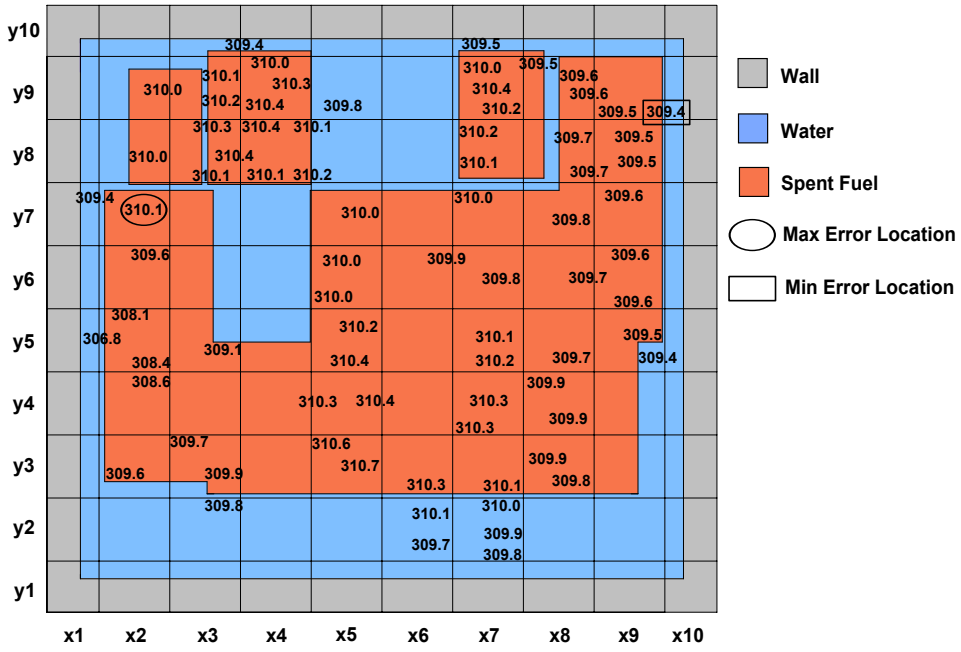

Fig. 6. TRACE temperatures (K) at 4.36 meters from the bottom.

corresponds to Section A-A of the Fig. 2. This section contains a considerably fraction of cycle 6 fuel and it is where more residual heat is generated. Fig. 9 and Fig. 10 show the measured and predicted temperatures for this zone, respectively. We can observe that the temperatures are quite similar, but the TRACE temperatures overpredict the experimental values about $0.2 - 0.4K$ at the upper levels. However, TRACE overall performance is quite good as the average error calculated is 0.092%, with a maximum error of 0.42%, and

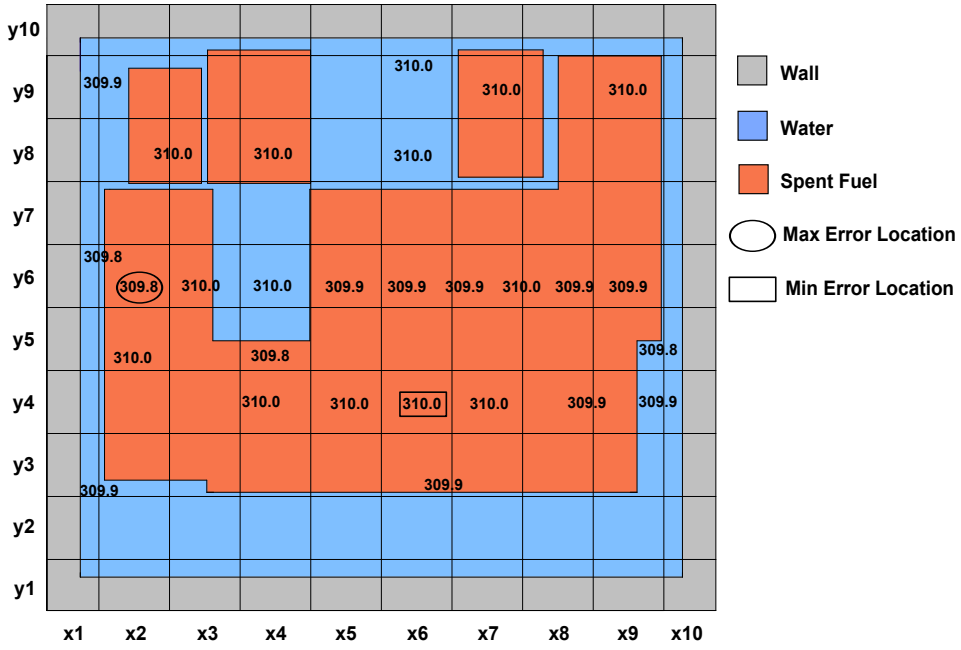

Fig. 7. Measured temperatures (K) at 10.72 meters from the bottom.

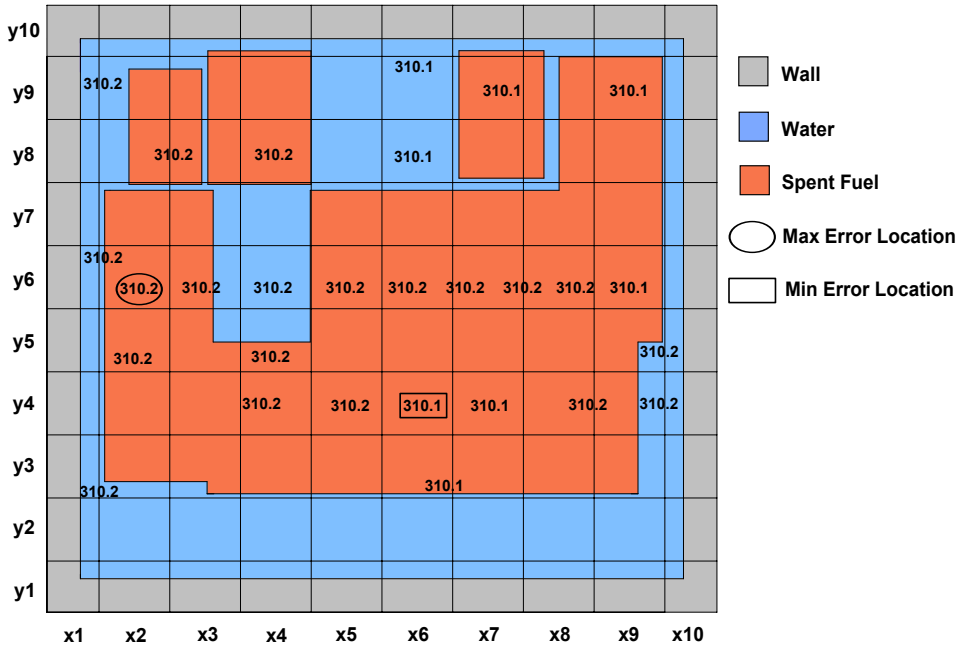

Fig. 8. TRACE calculated temperatures (K) at 10.72 meters from the bottom.

a mimimum error of 0%,. The location od the maximum and minimum error is marked Fig. 9 and Fig. 10 with a circle and a square, respectively.

Finally, Fig. 11 shows the experimental and calculated averaged-level coolant temperatures distribution with the elevation. We can observe more clearly this overprediction, although the values are quite close.

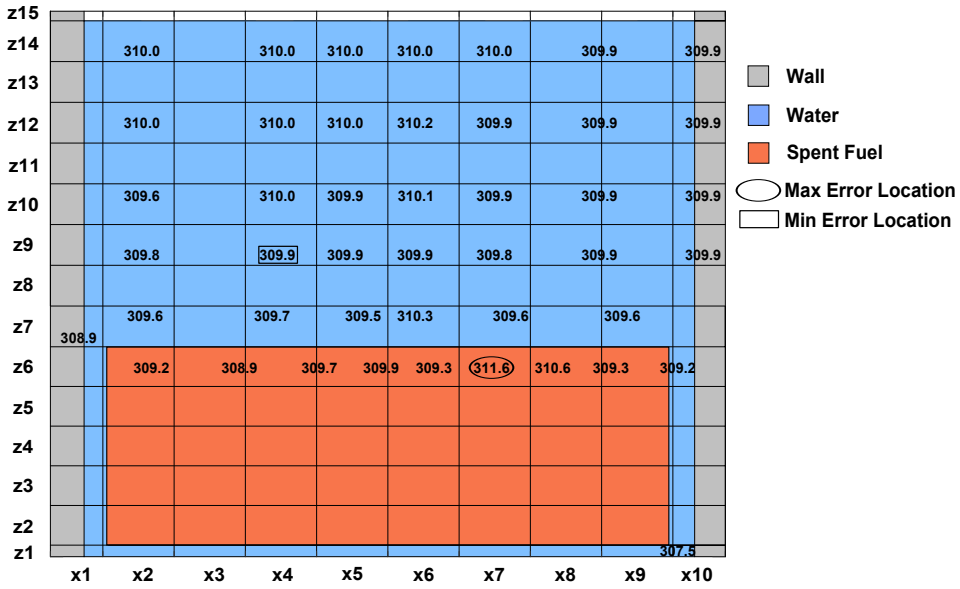

Fig. 9. Measured temperatures (K) at section A-A of the Fig. 2.

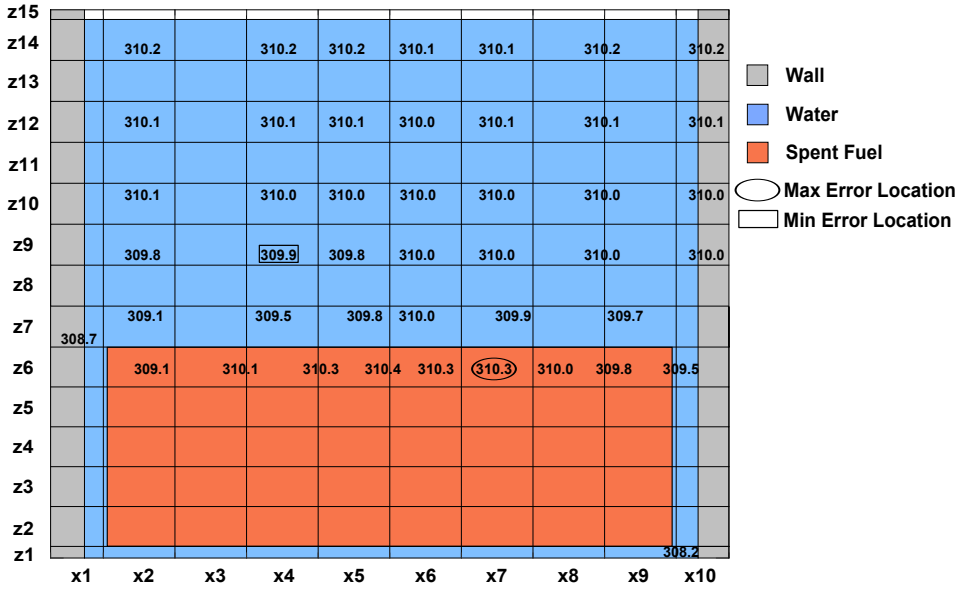

Fig. 10. TRACE calculated temperatures (K) at section A-A of the Fig.2.

2.3 Licensing case

In order to further analyze if the model proposed for TRACE is adequate for spent fuel storage pool simulation, a calculation of the Maine Yankee spent fuel pool licensing case was performed. The major difference of this new case with the former one is the power distribution inside the pool. In the licensing case it is assumed that the pool is working under the worst possible operation conditions. In particular, two regions are considered inside the pool, distributed as shown in Fig. 12. The one labeled as "hot elements" is constituted by a

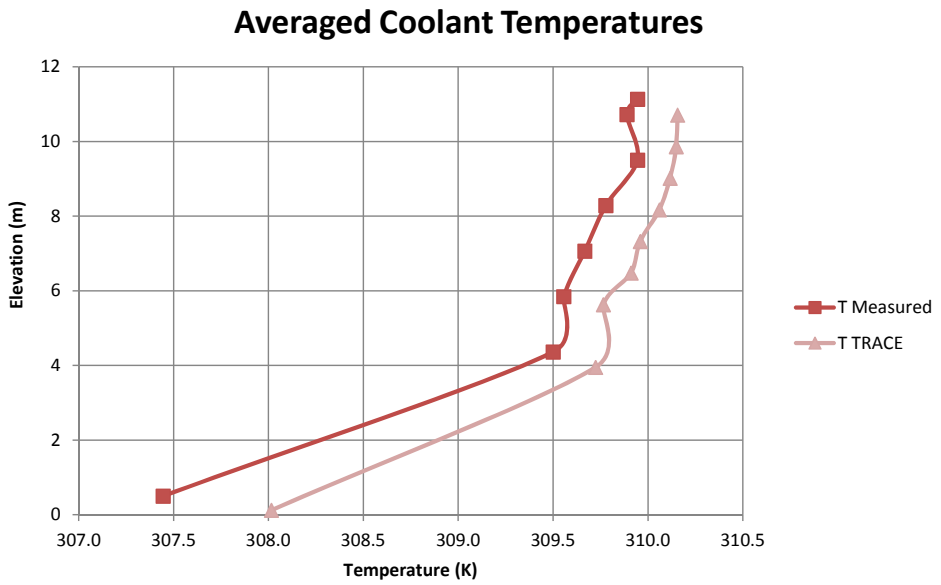

Fig. 11. Averaged coolant temperatures (K).

group of 70 elements that generate a residual heat of 4.8 MW, the rest of the spent fuel assemblies generate 6.4 MW. The temperature inside the pool is maintained with a coolant mass flow rate of 97.6 kg/s with a temperature of 324.7 K.

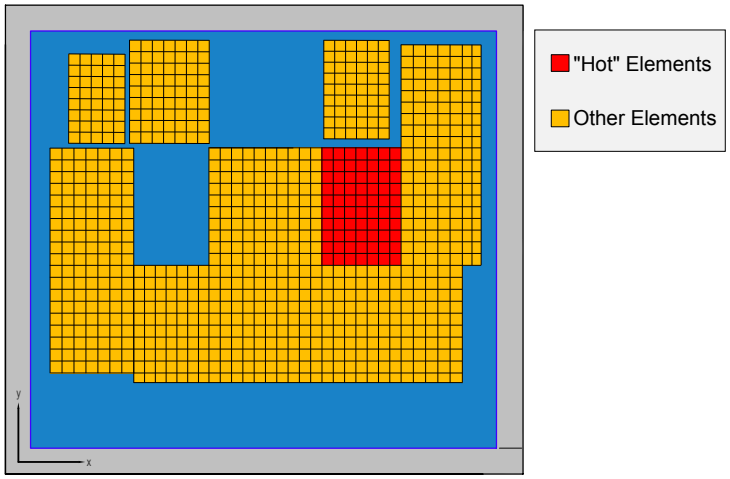

Fig. 12. Spent fuel distribution in Maine Yankee Spent Pool at licensing case.

Table 2 shows the comparison of the results calculated by TRACE with the results obtained from references (Gay and Gloski , 1983) and (Gay , 1984) calculated with GFLOW. In this case, TRACE predictions also agree with the results of GFLOW code.

Table 2
Licensing case comparison results between GFLOW and TRACE codes.

	GFLOW	TRACE
Maximum fluid temperature in poo (K)	345	345.8
Average temperature at bottom of pool (K)	340	339.7
Average temperature at pool top surface (K)	342	344.6
Average coolant exit temperature (K)	341	340.5
Temperature rise through hot assembly (K)	5	5.5

3 Estimation of thermal-radiation model parameters

Above a temperature threshold thermal-radiation heat transfer becomes important and affects the evolution of the clad temperatures. TRACE code has implemented a model to calculate thermal-radiation heat transfer (USNRC , 2010a) (USNRC , 2010b), which is incorporated into a new component named RADENC. This model is based on the radiation-enclosure method that evaluates radiative exchanges between discrete surfaces of heat structure (HTSTR) components that may be convection heat-transfer coupled to particular hydraulic component cells. The model implemented in RADENC component only calculates radiation heat transfer between the surfaces of the same axial level, what means that no axial radiation heat transfer is considered. For each axial level heat transfer is calculated only if the following criteria are satisfied:

(1) At least one heat structure of the convective surfaces contained within the radiation heat transfer enclosure must be in post-CHF heat transfer mode.
(2) The maximum difference between wall temperature and saturation temperature for all the heat structure surfaces contained within the radiation heat transfer enclosure must be grater that 100 K.
(3) The difference between the maximum and the minimum surface temperature within the radiation heat transfer enclosure must be greater than 10 K.

When these criteria are met the heat transferred by radiation is significant and it has to be taken into consideration. RADENC component needs data of emissivity, and geometric factors, beam lengths and view factors, to compute the thermal-radiation heat transferred. In this work, the thermal radiation heat transfer model is activated at the “hot elements” location, see Fig. 12, as is in this part of the spent fuel pool where the conditions to consider a significant radiation heat transfer are met. The spent fuel rack is made of aluminium and in each one of its vertical channels contains a 14x14 fuel rod spent fuel assembly. As the spent fuel assemblies are in separated rack channels

there is no possibility of radiation heat transfer between two different fuel assemblies. The thermal-radiation heat exchange will take place inside the channels and the radiative surfaces will be the spent fuel rods and the storage rack walls that contains the fuel assembly. Considering the geometry shown in Fig. 13 an input of RADGEN code of the COBRA thermal-hydraulic package (Rector , 1987) was constructed to calculate the view factors and path lengths between the different rods and the storage rack walls.

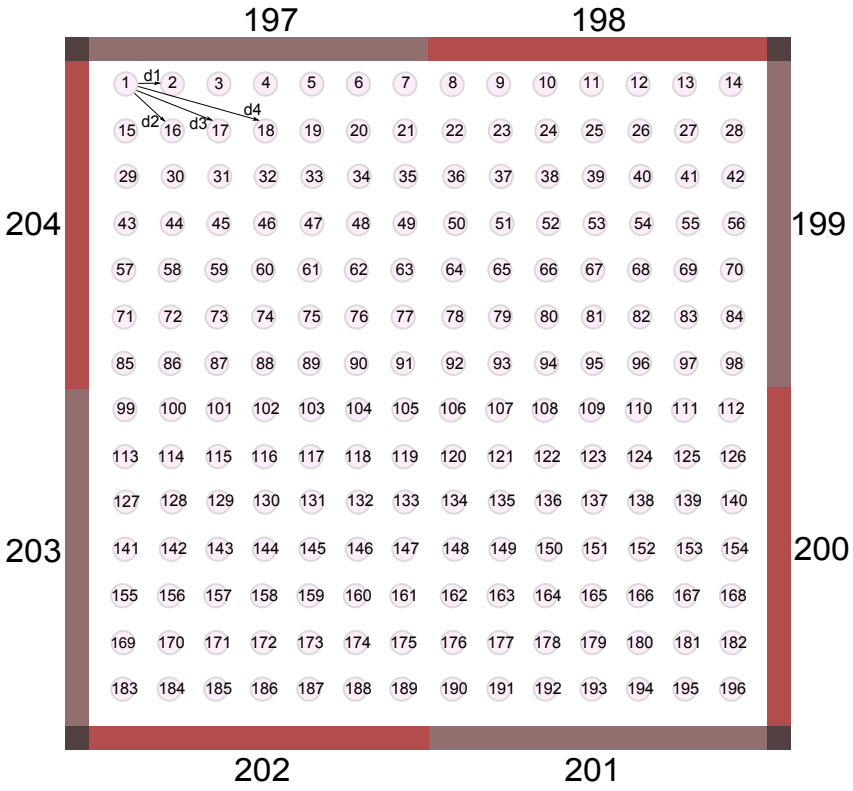

Fig. 13. RADGEN geometry.

RADGEN calculates the view factors among the 204 nodes that constitute the geometry exposed in Fig. 13. As an example Table 3 presents the view factors among the nodes that represent the spent fuel rack walls. It can be observed that as all the nodes are identical the values of the view factors of a node with himself are the same, and the reciprocity is satisfied, that is $F_{ij} = F_{ji}$ being i and j two nodes of the RADGEN geometry.

RADENC component does not compute radiation heat transfer pin by pin, so from the values computed by RADGEN, grouped view factors and path lengths have been obtained using the methodology indicated in TRACE manual (USNRC , 2010b). RADENC component only considers two radiative surfaces: Enclosure and fuel rods. The enclosure surface is constituted by the RADGEN nodes that simulate the canister walls, that is nodes from 197 to 204. The other RADGEN nodes, from 1 to 203, constitute the fuel rods radiative surface. Thus, taking as data the view factors calculated by RADGEN

Table 3
View factors between the spent fuel rack wall nodes.

NODES	197	198	199	200	201	202	203	204
197	9.32E-02	3.96E-03	4.43E-08	1.78E-13	3.40E-19	4.51E-14	4.43E-08	3.81E-02
198	3.96E-03	9.32E-02	3.81E-02	4.43E-08	4.51E-14	3.40E-19	1.78E-13	4.43E-08
199	4.43E-08	3.81E-02	9.32E-02	3.96E-03	4.43E-08	1.78E-13	3.40E-19	4.51E-14
200	1.78E-13	4.43E-08	3.96E-03	9.32E-02	3.81E-02	4.43E-08	4.51E-14	3.40E-19
201	3.40E-19	4.51E-14	4.43E-08	3.81E-02	9.32E-02	3.96E-03	4.43E-08	1.78E-13
202	4.51E-14	3.40E-19	1.78E-13	4.43E-08	3.96E-03	9.32E-02	3.81E-02	4.43E-08
203	4.43E-08	1.78E-13	3.40E-19	4.51E-14	4.43E-08	3.81E-02	9.32E-02	3.96E-03
204	3.81E-02	4.43E-08	4.51E-14	3.40E-19	1.78E-13	4.43E-08	3.96E-03	9.32E-02

the value of four grouped view factors have to be calculated corresponding to the couples: enclosure-enclosure, enclosure-rods, rods-enclosure and rods-rods. The general expression to obtain a grouped view factor is given by:

$$FG_{mn} = \frac{\sum\limits_{i \in ms} A_i \sum\limits_{j \in ns} F_{ij}}{A_m} \ , \tag{1}$$

where A_i is the area of node i, F_{ij} is the view factor between node i and j calculated by RADGEN code, ms and ns are the sets nodes that constitute a radiative surface, enclosure or fuel rods, and A_m is the sum of the individual areas of the nodes corresponding to ms group.

In order to maintain the conservation of the thermal radiated energy from a radiative surface, it has to be satisfied that

$$\sum_{n=1}^{N} FG_{nm} = 1 \ , \tag{2}$$

where N is the number of radiative surfaces involved in the thermal-radiation exchange. Finally, the reciprocity should be satisfied, that is the energy radiated by the m-th group to the n-th group is the same as the energy collected by the n-th from the m-th group. This is expressed as

$$A_m FG_{mn} = A_n FG_{nm} \ , \tag{3}$$

As RADENC only considers two radiative surfaces, enclosure and rods, four grouped view factors have to be obtained corresponding to the pairs: Enclosure-

Table 4
RADENC grouped view factors.

Surfaces	View factor
Enclosure-enclosure	0.135256149
Enclosure-rods	0.864743851
Rods-enclosure	0.132696376
Rods-rods	0.867303624

enclosure, enclosure-rods, rods-enclosure and rods-rods. To calculate these values we proceeded as follows: Considering the values exposed in Table 3, corresponding to the view factors of the pairs of nodes that constitute the enclosure, and their area and using them in Eq. (1) the enclosure-enclosure grouped view factor was calculated. Then, applying Eq. (2) to guarantee the thermal radiate energy conservation in the enclosure, the enclosure-rods grouped view factor is obtained. Next, applying the reciprocity requirement given by Eq. (3) The rods-enclosure grouped view factor is calculated. Finally, the rods-rods grouped view factor is obtained by applying again Eq. (2). Table 4 present the values of the four grouped view factors.

RADENC also needs the grouped path lengths between the radiative surfaces, which are computed using the expression

$$LG_{mn} = \frac{\sum_{i=ns} A_i \sum_{j=ms} F_{ij} L_{ij}}{A_m FG_{mn}} \tag{4}$$

where A_i is the area of node i, F_{ij} and L_{ij} are the view factor and the distance between node $i$and j, respectively, ns is the set of nodes associated with the n-th group, and ms is the set of nodes associated with the m-th group, enclosure or rods, FG_{mn} is the corresponding grouped view factor calculated and A_m is the total area of the nodes corresponding to the m-th group.

In this work, the calculations are performed using the distances exposed in Fig. 13. The consideration of more separated nodes does not provide a significant difference on the grouped path length value calculated. Table 5, shows the values of all grouped path lengths to be used in RADENC component.

Finally, RADENC component also requires the emissivity coefficients of the enclosure and rod materials. Maine Yankee spent fuel storage racks material is aluminium with an emissivity of 0.55 and for the spent fuel rods an emissivity of 0.8 is taken, as it is recommended in reference (Adkins et al., 2009), for PWR fuel rods.

As explained previously, the activation of thermal-radiation model requires some conditions that are not met in the stationary situations studied, but

Table 5
RADENC grouped path lenghts.

Surfaces	Path lengths
Enclosure-enclosure	0.00915
Enclosure-rods	0.02454
Rods-enclosure	0.02454
Rods-rods	0.03594

they are met in some accidental sequences. One of such sequences consists of considering as initiating event the loss of spent fuel pool cooling together with the loss of coolant through the transfer channel. Once the initiating event is produced the worst scenario possible is to consider that no accident mitigating actions are taken, and this accidental sequence is the one studied in section 4.

4 Transient simulation.

Several accidents in spent fuel pools have been identified and some of them even taken place in commercial nuclear power plants (Boyd, 2000) (Ibarra et al. , 1997) (Throm , 1989). Among the accidental sequences that could occur, there is the transient initiated by a loss of the spent fuel cooling system together with a loss of coolant through the transfer channel, considering that no accident management measures are taken to mitigate the accident consequences. This transient has been simulated for Maine Yankee spent fuel pool at licensing conditions.

Fig. 14 shows a scheme of the events that occur in such accidental sequence. Thus, when the transient starts, the residual heat generated by the fuel assemblies makes the water temperature to increase up to 373 K when boiling conditions are reached. At this time the evaporation of the spent fuel pool coolant starts and the spent fuel pool level decreases. When uncovering of the assemblies is produced the fuel temperature rises and first, oxidation of the fuel is produced and hydrogen generation starts. After that, the maximum peak cladding temperature is reached and melting of spent fuel takes place. In this transient, temperatures around 1000 K are reached in the spent fuel elements and, at such conditions; the heat exchanged by thermal radiation can be important and can affect the evolution of plant safety variables. Thus, two runs were performed in one of them no thermal-radiation is considered and in the other the TRACE thermal-radiation exchange model is activated using the parameters estimated in section 3.

The available time to mitigate the accident depends on the mass of water inside

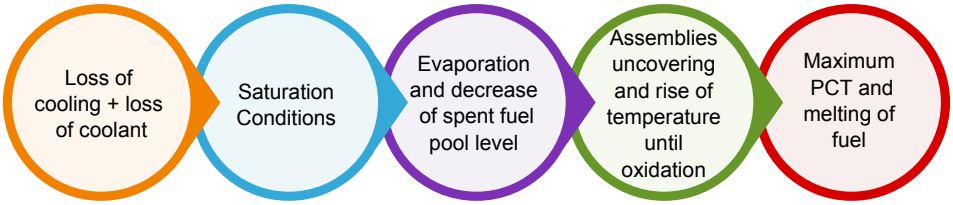

Fig. 14. Events after the loos of spent fuel cooling system.

the pool at the start of the transient. In this case we consider the coolant is lost through the transfer channel, so there is a sudden decrease in the spent fuel pool level until it reaches 20 cm of water above the spent fuel assemblies. In this situation the residua power generated by the spent fuel assemblies start to heat the remaining coolant inside the spent fuel pool.

Thus, taking as initial data, for residual power and temperatures, the values of the steady state previously calculated for the licensing case, the time needed to reach saturation conditions, ts, can be obtained by a simple energy balance equation given by

$$t_s = \frac{mC_p\Delta T}{Q} \ , \tag{5}$$

where m is the total mass water inside the pool after the break is produced, $Q = 6.4$ MW is the total residual heat generated, $C_p = 4181$ J/(kg K), and ΔT is the difference between initial coolant and saturation temperatures.

In an analogous way, the time to uncover the fuel assemblies can be calculated assuming that the heat from the spent fuel pool is removed only by evaporation of water, and can be calculated by

$$t_u = \frac{\Delta V}{v\, ws} \ , \tag{6}$$

where ΔV is the volume of water above the spent fuel assemblies, $\Delta V = 28476$ m^3; v is the specific volume water in the pool, $v = 0.001$ m^3/kg, and ws is the evaporation rate, which is calculated in this work as

$$ws = \frac{Q}{(h_s - h_b)} \tag{7}$$

where $Q = 6.4$ MW is the total residual heat generated, is the steam enthalpy at saturation conditions, $h_s = 2676$ KJ/kg, and h_b is the water boiling enthalpy at 373 K, $h_b = 419$ KJ/kg. Assuming these values are constant the evaporation rate calculated by Eq. (6) is $ws = 4.125$ kg/s. Table 6 presents the analytical and TRACE calculated times until saturation and time until spent fuel assemblies uncovering. The time calculated by TRACE is slightly larger than the one obtained with the simplified calculation, but this is due to the simplifying assumptions of the analytical model. Thus, for example, in the analytic calculation adiabatic conditions are assumed, what is not considered in TRACE.

Table 6
Time until saturation conditions and fuel assemblies uncover.

	Time until saturation (s)		Time to uncover spent fuel assemblies (s)	
	t_s		$t_u + t_s$	
	Analytic result	TRACE	Analytic result	TRACE
Loss of cooling + loss of coolant	11520	12025	21562	21777

The evolution of the spent fuel coolant temperature until saturation calculated by TRACE is presented in Fig. 15. It can be observed that there is a constant rise in the coolant temperature due to the residual heat generated by the spent fuel assemblies. When water starts boiling, the spent fuel pool level decreases due to evaporation. Fig. 16 shows the evolution of the averaged spent fuel pool level calculated by TRACE. There is a slight increase in the level due to the change in coolant density, but it decreases by evaporation. In this phase of the transient, as the temperature in the clad is kept about 400 K, as shown in Fig. 17, thermal-radiation heat transfer model is not activated, so the evolution of the coolant temperature is identical for both runs.

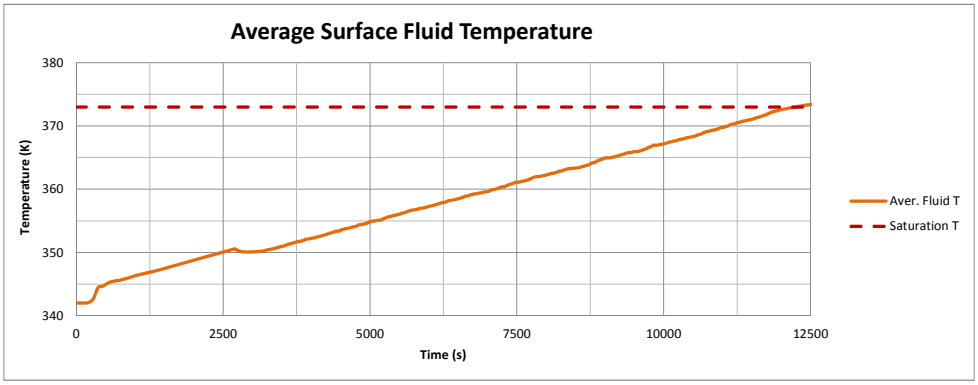

Fig. 15. Water temperature until saturation conditions.

Fig. 17 shows the evolution of clad temperature of the hottest fuel assemblies for both runs. In this Figure is observed that when thermal-radiation model is activated, the total heat transferred by the fuel assembly to the coolant is higher than in the case this exchange is not considered, and the clad temperature is maintained at lower values. Thus, while in both cases the clad temperature rising starts at 62650 s, the predicted temperature values reached in the case of not considering the thermal-radiation model are higher than the ones obtained considering this model. In fact, for the clad temperature the limiting value for clad oxidation is reached at 68425 s while considering

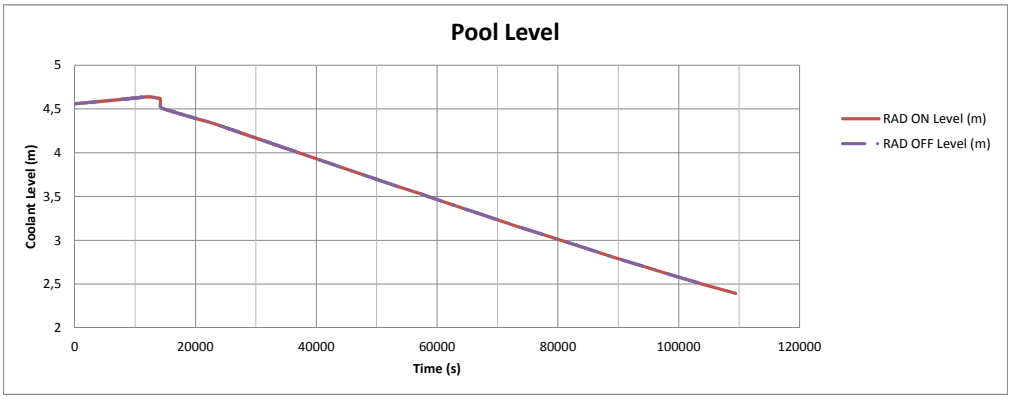

Fig. 16. Spent fuel pool collapsed level.

radiation exchange this temperature is not met until 100829 s, so this limit is delayed 32404 s. In an analogous way, the peak cladding temperature limit is 4225 s delayed if thermal radiation is considered, as shown in Fig. 17.

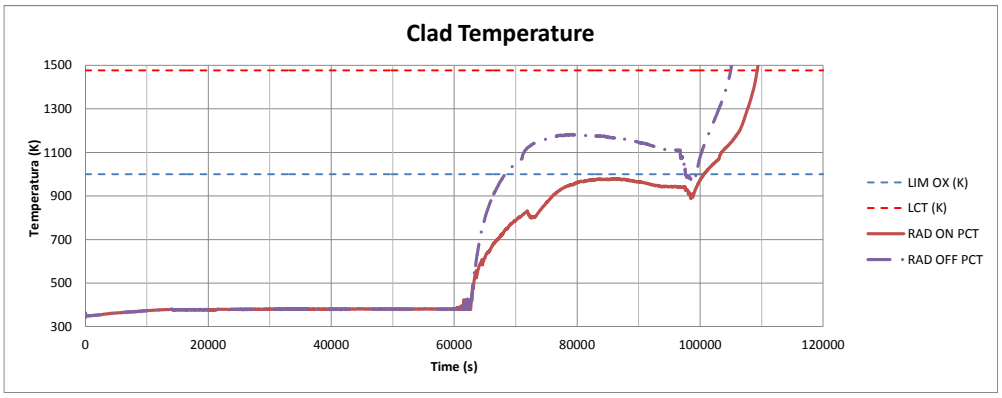

Fig. 17. Cladding temperature.

The delay in reaching the oxidation temperature makes has a direct effect on the time available until the maximum clad oxide thickness allowed in CFR 50.46 (USNRC , 2007) is met. The limiting value established in CFR 50.46 is 17% of the total clad thickness. Thus, Fig.18 shows the evolution of oxide thickness in the clad for both cases. It can be observed that there is a considerable difference in the time available until complete clad oxidation. In particular TRACE calculates a delay of 27479 s if radiation heat transfer model is activated.

The oxidation reaction produces hydrogen, which is also limited by CFR-50.46 (USNRC , 2007). Fig. 19 shows the amount of hydrogen produced along the transient and the limiting value established by CFR-50.46. In this case, it is also evidenced the difference in the evolution of hydrogen production. Thus, if no thermal-radiation is considered hydrogen production starts at 71076 s,

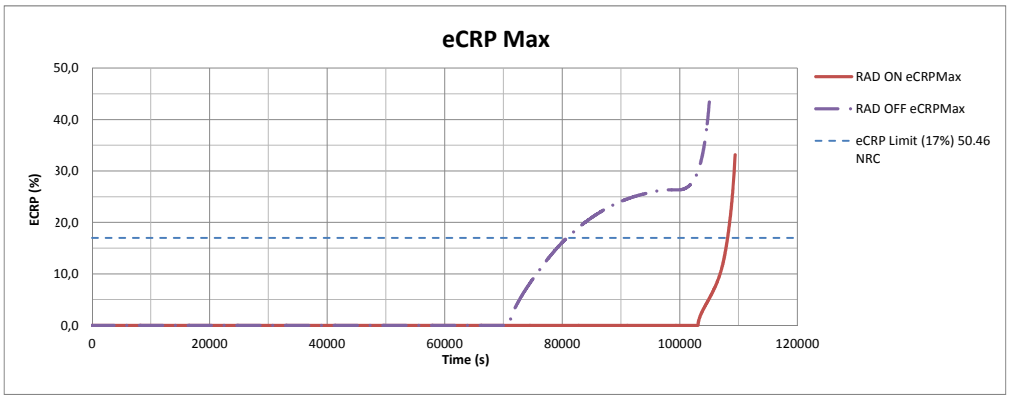

Fig. 18. Oxide thickness in the clad.

and considering this heat exchange the hydrogen production is delayed until 103179 s.

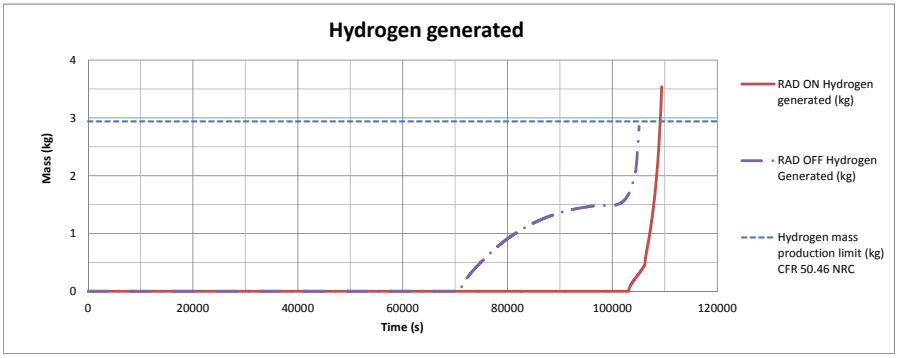

Fig. 19. Hydrogen produced along the transient.

The evolution of oxide thickness and hydrogen production are consistent with the evolution of the clad temperature, shown in Fig. 17, as the oxidation model implemented in TRACE code does not activate unless clad temperature is 1000 K. If thermal-radiation exchange is considered the clad temperature is lower and does not reach this threshold of temperature until 100829 s, so for the previous time TRACE does not calculate clad oxidation.

Finally, Table 7 presents a summary of the time of all the events identified since the start of the transient, for both runs. In this table it is observed the considerably available time gained until oxidation and peak cladding temperature if thermal-radiation exchange is considered.

Table 7
Timing of the main events.

	Thermal-radiation	
	ON	OFF
Saturation Conditions (s)	12025	12025
Spent fuel assemblies uncover (s)	21777	21777
Oxidation temperature (s)	100829	68425
Maximum peak cladding temperature (s)	109204	104979

5 Conclusions

Spent fuel pools safety analysis has become of great interest for regulatory bodies and for nuclear industry. As best estimate codes are widely used to perform nuclear safety analysis, it is interesting to assess the capability of such codes to simulate accidents regarding spent fuel pools. In this paper, a TRACE model for Maine Yankee spent fuel storage pool based on the use of VESSEL component is presented. This model has been used to perform a steady state calculation in order to compare the predicted calculations with experimental measurements. The comparison suggests that TRACE is an accurate, three-dimensional model that may have benefit in the licensing process by being able to remove engineering conservatisms traditionally used. Moreover, a transient considering the loss of cooling and de loss of coolant through the transfer channel has been simulated. For this application TRACE thermal-radiation model has been activated and the parameters needed have been estimated using RADGEN code. From the comparison between the results obtained, it has been evidenced the importance of considering the radiation-heat transfer, as important safety limits as clad oxidation, hydrogen production and peak cladding temperature present a considerably delay.

Acknowledgements

This work has been supported by the Consejo de Seguridad Nuclear under the contract with reference STN/2369/08/640.

References

Adkins, H. E., Cuta Jr. J. M., Koeppel B. J., Guzman A. D., Bajwa, C. S. 2009. Spent Fuel Transportation Package Response to the Baltimore Tunnel Fire Scenario (NUREG/CR-6886, Rev. 2). NUREG/CR-6886, Rev. 2.

Applied Programming Technology, Inc. 2012. Symbolic Nuclear Analysis Package (SNAP).User's Manual. Version 2.2.1.

Boyd, C.F. 2000. Predictions of Spent Fuel Heatup After a Complete Loss of Spent Fuel Pool Coolant. NUREG-1726

Carlos, S.; Villanueva, J.F.; Martorell, S., Serradell, V. 2008. Analysis of a loss of residual heat removal system during mid-loop conditions at PKL facility using RELAP5/Mod3.3. Nuclear Engineering and Design 238(10), 2561-2567.

Ferng, Y., Ma, S., 1996. Investigation of system responses of the Maanshan nuclear power plant to the loss of the heat removal during midloop operation using RELAP5/Mod3 simulation. Nuclear Technology 116, 160-172.

Gay, R.R., Gloski, D.M., 1983. Verification of the GFLOW Computer Code Using experimental Data from the Maine Yankee Spent-Fuel Storage Pool. EPRI NP-3097.

Gay, R.R., 1984. Spent Nuclear Fuel Storage Pool Thermal Hydraulic Analysis. Progress in Nuclear Energy, 14(3), 199-225.

Hassan, Y.A., Banerjee, S.S., 1994. RELAP5/Mod3 simulation of the loss of the residual heat removal system during a midloop operation experiment conducted at the ROSA-IV large scale test facility. Nuclear Technology. 118, 191-206.

Hassan, Y.A., Raja, L.L., 1993. Simulation of loss of RHR during midloop operation and the role of steam generators in decay heat removal using the RELAP5/Mod3 code. Nuclear Technology. 103, 310-318.

Hassan, Y.A., Troshko, A.A., 1997. Simulation of loss of the residual heat removal system of BETHSY integral test facility using CATHARE thermal-hydraulic code. Nuclear Technology 119 (1), 29-37.

Hung, T., Dhir, V., Pei, B., Chen, Y., Tsai, F. 2013. The development of a three-dimensional transient CFD model for predicting cooling ability of spent fuel pools. Applied Thermal Engineering 50, 496-504.

IAEA, 2007. Operation and Maintenance of Spent Fuel Storage and Transportation Casks/Containers. IAEA-TECDOC-1532.

Ibarra, J.G., Jones, W.R., Lanik, G.E, Ornstein, H.L., Pullani, S.V. 1997. Operating Experience Feedback Report. Assessment of Spent Fuel Cooling. NUREG 1275 Vol.12.

Kaliatka A., Ognerubov, V., Vileiniskis, V. 2010. Analysis of the processes in spent fuel pools of Ignalina NPP in case of loss of heat removal. Nuclear Engineering and Design 240, 1073-1082.

Lee, C.M., Lee, K.J. 2007. A study on operation time periods of spent fuel interim storage facilities in South Korea. Progress in Nuclear Energy 49, 323-333.

Rector, D. R. 1987. RADGEN: A radiation exchange factor generator for rod bundles. Pacific Northwest Laboratory.

Rogers, K.A. 2009. Fire in the hole: A review of national spent nuclear fuel disposal policy. Progress in Nuclear Energy 51 (2009) 281-289.

Throm, E.D., 1989. Regulatory Analysis for the Resolution of Generic Issue

82, Beyond Design Basis Accidents in Spent Fuel Pools. NUREG-1353
USNRC. 2007. CFR.50.46.NRC: Acceptance criteria for emergency core cooling systems for light-water nuclear power reactors. USNRC.
USNRC. 2010a. TRACE V5.0 THEORY MANUAL Field Equations, Solution Methods, and Physical Models. U. S. Nuclear Regulatory Commission, Washington, DC 20555-0001.
USNRC. 2010b. TRACE V5.0 USER'S MANUAL Volume 2: Modeling Guidelines. U. S. Nuclear Regulatory Commission, Washington, DC 20555-0001.
Vihavainen, J., Riikonen, V., Kyrki-Rajamäki, R. 2010. TRACE code modeling of the horizontal steam generator of the PACTEL facility and calculation of a loss-of-feedwater experiment. Annals of Nuclear Energy 37, 1494-1501.
Villanueva, J. F.; Carlos, S.; Martorell, S. Serradell, V., Pelayo, F., Mendizabal, R. 2008. Availability of alternative sources for heat removal in case of failure of the RHRS during midloop conditions addressed in LPSA. European Safety and Reliability Conference (ESREL)/17th Annual Meeting of the Society-for-Risk-Analysis-Europe (SRA-Europe). Valencia, Spain September 22-25.
Wang. J.R., Lin, H.T., Cheng Y.H., Wang, W.C., Shih, C. 2009. TRACE modeling and its verification using Maanshan PWR start-up tests. Annals of Nuclear Energy 36, 527-536.
Wang, J.R., Lin, H.T., Tseng Y.S., Shih, C. 2012. Application of TRACE and CFD in the spent fuel pool of Chinshan nuclear power plant. Applied Mechanics and Materials 145, 78-82.
Watanabe T., Ishigaki, M., Hirano, M. 2012. Analysis of BWR long-term station blackout accident using TRAC-BF1. Annals of Nuclear Energy 49 223-226.